High-Resolution Technetium-99m-HMPAO SPECT in Patients with Probable Alzheimer's Disease: Comparison with Fluorine-18-FDG PET

Cristina Messa, Daniela Perani, Giovanni Lucignani, Arturo Zenorini, Felicia Zito, Giovanna Rizzo, Franco Grassi, Angelo Del Sole, Massimo Franceschi, Maria Carla Gilardi and Ferruccio Fazio

INB-CNR, University of Milano, Institute H.S. Raffaele, Milano, Italy

SPECT studies of regional cerebral perfusion with a high-resolution system were compared to PET studies of regional cerebral glucose utilization (rCMRglc) in 21 patients with probable Alzheimer's disease (AD). Ten normal subjects were also evaluated with SPECT and 10 with PET. **Methods:** rCMRglc (for PET) and counts (for SPECT) in the associative cortices were normalized to the average rCMRglc, and counts in the calcarine cortex and basal ganglia were considered as a "reference area" to obtain a ratio. The ratio differences between patients and controls were tested with ANOVA performed separately for PET and SPECT. **Results:** The difference between probable AD patients and controls was significant for both PET ($p < 0.00001$) and SPECT ($p < 0.005$); this difference was significant for the frontal, temporal and parietal cortices ($p < 0.0001$) for PET, and for the temporal ($p < 0.005$) and parietal ($p < 0.001$) cortices for SPECT. Temporo-parietal defects were detected in all subjects with PET and in 90% with SPECT. **Conclusion:** PET and SPECT are able to detect characteristic temporo-parietal abnormalities in probable AD. However, the presence of abnormalities in other associative areas is better evaluated with PET.

Key Words: single-photon emission computed tomography; positron emission tomography; Alzheimer's disease; fluorine-18-fluorodeoxyglucose

J Nucl Med 1994; 35:210–216

The assessment of cerebral perfusion with SPECT is being increasingly used in the routine clinical evaluation of neurological and psychiatric disorders (*1*).

The clinical relevance of SPECT studies in the evaluation of patients with probable Alzheimer's disease in the early phase is related to the evidence of an abnormal pattern of perfusion (i.e., hypoperfusion of the temporo-parietal cortex) consistently detected by SPECT studies of blood flow in these patients (*2–6*). Although other patterns, such as frontal hypoperfusion and asymmetric involvement of the cerebral cortex have been observed (*7,8*), the presence of hypoperfusion in the temporo-parietal areas demonstrated by SPECT and ^{99m}Tc-hexamethyl propylenamine oxime (^{99m}Tc-HMPAO) has a high predictive value for the presence of AD in patients with memory and cognitive impairment (*8*).

The use of SPECT in clinical practice is facilitated by its lower costs and its wide diffusion compared to other techniques such as PET. On the other hand, the reliability of SPECT findings has always been limited by the relatively poor spatial resolution of circular shaped rotating gamma cameras and the low brain uptake values of the tracers used (*9*). With the development of new high-resolution SPECT systems, both spatial resolution and detection efficiency of tomographic imaging are improved compared to single-head rotating gamma camera systems (*10*), thus allowing a better image quality and improving the quantification of regional radioactivity. However, the improvement in image quality obtained by high-resolution SPECT does not diminish the limitations related to the kinetics of the tracers used (*11*).

PET is a more accurate technique than SPECT with regard to resolution and quantitative accuracy (*12,13*) and it should be regarded as the reference technique for the assessment of regional brain function. A reduction of glucose metabolism measured with PET and ^{18}F-fluoro-2-deoxy-D-glucose (^{18}F-FDG) in the temporo-parietal cortex has been consistently shown in patients with mild to moderate probable AD (*14–16*), although other patterns of glucose metabolism such as frontal (*17*) or asymmetric involvement of the cerebral cortex (*18–21*) have also been observed. Although PET has been successfully used to assess the metabolic function in patients with probable AD, its applicability to clinical practice is limited by the high costs; indeed PET has now been mostly used for research purposes.

The aim of this study was to carry out a systematic evaluation of PET versus SPECT in patients with early AD

Received Jun. 14, 1993; revision accepted Oct. 20, 1993.

For reprints and correspondence contact: Cristina Messa, MD, Medicina Nucleare, Istituto H San Raffaele, Via Olgettina 60, 20132 Milano, Italy.

TABLE 1
Patients' Clinical Data

Patient no.	Sex	Age (yr)	Duration of disease (mo)	MMSE	MRI	Δt PET/ high-resolution SPECT (days)
1	F	59	12	20	Atrophy	2
2	M	57	24	19	Atrophy	57
3	M	57	24	16	Normal	6
4	M	67	36	22	Atrophy + wm	1
5	M	62	24	20	Atrophy	1
6	M	60	12	15	Atrophy	28
7	F	70	5	14	Atrophy	12
8	F	77	24	25	Atrophy	2
9	F	73	29	29	Atrophy	6
10	F	74	24	21	Wm	1
11	M	57	24	24	Atrophy	2
12	M	66	36	19	Atrophy	6
13	F	52	12	22	Atrophy + wm	1
14	M	64	36	14	Atrophy	1
15	F	60	24	23	Normal	4
16	M	63	24	23	Atrophy	8
17	F	62	6	29	Atrophy	1
18	F	44	24	14	Normal	88
19	M	68	36	24	Atrophy	1
20	F	69	24	12	Atrophy	11
21	F	58	36	12	Atrophy	6

MMSE = mini mental state examination; Δt = time elapsed between PET and SPECT studies; Atrophy = mild degree of atrophy; wm = small lesions of the white matter.

with the purpose of evaluating, in the same patients, the relative ability of high-resolution SPECT with ^{99m}Tc-HMPAO in comparison with PET and ^{18}F-FDG to differentiate patients in the early phase of the disease from normal controls and to detect abnormalities that are considered characteristic of probable AD patients, such as temporoparietal impairment.

MATERIALS AND METHODS

Subjects

Twenty-one patients with probable AD (10 males, 11 females, mean age 62.8 ± 7.8 yr) were studied. The main clinical and radiological features of these patients are reported in Table 1.

All patients were clinically diagnosed as probable AD (average duration of illness 23.6 ± 9.6 mo) according to standard criteria (*22*). Other causes of dementia were excluded through neurological examination and laboratory blood tests. The severity of the disease, assessed with the Mini Mental State Examination (MMSE), was mild to moderate (MMSE mean score 19.8 ± 5; Table 1).

An MRI study was performed in all patients with a 1.5 T scanner (Magnetom, Siemens, Enrlangen, Germany). A mild degree of generalized atrophy was observed in 16/21 patients and small lesions of the white matter, probably due to vascular lacunar lesions, were present in 3/21 patients (Table 1).

At the time of the PET and high-resolution SPECT examinations, patients were free from pharmacological treatments known to alter cerebral perfusion and metabolism.

All patients underwent a PET study with ^{18}F-FDG and a high-resolution SPECT study with ^{99m}Tc-HMPAO. The average time between PET and high-resolution SPECT examinations was 11.7 ± 21.7 days (Table 1) and the order of the exams was random.

Normal controls for the PET study were 3 males and 7 females (mean age 47 ± 13 yr), while normal controls for the high-resolution SPECT study were 4 males and 6 females (mean age 53 ± 13 yr). All controls were free from known neurological diseases, including cerebrovascular disease as assessed by clinical history, standard clinical and neurological examinations and neuropsychological testing (MMSE).

The protocol was approved by the Ethics Committee of the Scientific Institute H. San Raffaele. Informed consent was obtained from each subject.

PET Imaging

PET studies were performed with a PET tomograph (931/04-12 CPS/Siemens, Erlangen, Germany) with a spatial resolution equal to 6.3 mm full width at half maximum (FWHM) in the axial image plane. The tomograph had an axial field of view of 5.4 cm which yielded seven axial image slices 6.75 mm thick (*23*).

The patients rested on the bed in a dim room, eyes open and ears unplugged, with their head positioned in a special head-holder which uses the subject's dental morphology for positioning and fixation (*24*). In some patients, a personal molded foam was used to fix the head.

The synthesis and quality control of ^{18}F-FDG was carried out according to standard procedures (*25*). Fourteen images, parallel to the orbito-meatal line, were acquired 45 min after the intravenous injection of approximately 250–300 MBq of ^{18}F-FDG with two spatially contiguous emission scans, each lasting 10 min, in order to examine the whole brain. During scanning, approximately 14 million counts were acquired.

Axial slices were reconstructed employing a Hann filter with a cut-off frequency of 0.5 cycles/pixel (matrix 128 × 128). Photon attenuation was corrected by use of coefficients determined from two transmission scans, one for each bed position, obtained with a ^{68}Ge/^{68}Ga external ring source, lasting 10 min each, prior to the ^{18}F-FDG injection.

Plasma ^{18}F-FDG and glucose time-activity curves (input functions) were obtained by blood sampling from the radial artery at approximately 3-sec intervals for the first minute after injection and at progressively longer intervals for the duration of the entire study.

Values of regional cerebral metabolic rate of glucose (rCMRglc) were calculated according to the method based upon the autoradiographic technique of Sokoloff et al. (*26*) and revised by Reivich et al. (*27*) for human PET studies.

High-Resolution SPECT Imaging

High-resolution SPECT imaging was performed with an annular SPECT system (CERASPECT—Digital Scintigraphic Inc., Maynard, MA) (*28*) with a spatial resolution equal to 8.4 mm FWHM in the center of the axial plane. The system covered an axial field of view of 10.5 cm. As with PET, the patients rested on a bed in a quiet room at the time of injection. The patient's head was positioned in a head-holder specifically built for the CERASPECT machine.

Images parallel to the orbito-meatal line were acquired beginning 15 min after intravenous injection of approximately 740–800 MBq of ^{99m}Tc-HMPAO. In 30 min, 7 to 9 million total counts were acquired for the entire head, using a square pixel size equal to 1.66 mm and an angular step of 3° over 360° (matrix size 128 × 64 and 120 projections).

TABLE 2
PET and High-Resolution SPECT Ratio Values (°) in Probable Alzheimer's Disease Patients and Normal Controls

Region	PET AD	PET N	SPECT AD	SPECT N
Associative frontal	0.796 ± 0.092*	0.962 ± 0.024	0.828 ± 0.102	0.887 ± 0.034
Mesial frontal	0.792 ± 0.071*	0.933 ± 0.043	0.871 ± 0.092	0.889 ± 0.054
Temporal	0.708 ± 0.061*	0.830 ± 0.057	0.839 ± 0.076†	0.910 ± 0.034
Parietal	0.704 ± 0.080*	0.943 ± 0.030	0.838 ± 0.101‡	0.960 ± 0.040
Lateral occipital	0.826 ± 0.116	0.918 ± 0.073	0.983 ± 0.109	1.026 ± 0.046
Thalamus	0.958 ± 0.074	0.951 ± 0.054	1.031 ± 0.086	0.995 ± 0.080
Cerebellum	0.830 ± 0.082	0.856 ± 0.042	1.198 ± 0.12	1.154 ± 0.075

(°) = Left and right hemispheres ratios are averaged. AD = Alzheimer's disease; N = normal controls.
* = $p < 0.0001$.
† = $p < 0.005$.
‡ = $p < 0.001$.

Sixty-four axial slices, 1.66 mm thick, were reconstructed using a Hann filter with a cut-off frequency of 0.5 cycles/pixel. The reconstructed images were corrected for attenuation with the Chang's first order method (*29*) with an attenuation coefficient equal to 0.1 cm^{-1}. Four consecutive axial slices were added together in order to obtain a slice thickness of 6.64 mm, similar to that of the PET images.

Data Analysis

PET and high-resolution SPECT image analysis was performed on a SUN (SPARC) workstation. Circular regions of interest (ROIs, diameter = 1.5 the FWHM of the respective system) were manually positioned on all the cortical and subcortical structures and on the cerebellar hemispheres. Mean rCMRglc values (for PET) and mean counts (for SPECT) were calculated for each ROI and these values were simply averaged to obtain values of nine anatomo-functional areas identified according to the Damasio and Damasio atlas (*30*). This atlas is particularly suitable to examine cortical activity of associative areas (typically damaged in AD) and it has been previously used to evaluate PET and SPECT patterns in patients with cognitive deficits (*31,32*). The areas examined were the associative frontal, mesial frontal, temporal, parietal, lateral occipital and calcarine cortices, the thalamus, the basal ganglia (head of caudate and putamen) and the cerebellar cortex. Since the calcarine cortex and basal ganglia are generally spared in probable AD (*33*), mean rCMRglc and mean counts of the calcarine cortex and the basal ganglia were taken as the least affected areas and averaged to obtain a reference value (Aref) for normalization of brain activity. Data were then analyzed in the form of ratios determined as follows:

$$\text{Ratio} = \text{Ar}/\text{Aref},$$

where Ar equals rCMRglc for PET studies and counts for high-resolution SPECT studies in each anatomo-functional region, and Aref equals average rCMRglc for PET studies and average counts for high-resolution SPECT studies in the reference areas, i.e., the calcarine cortex and the basal ganglia.

Statistical Analysis

PET and high-resolution SPECT ratio values obtained in probable AD patients were compared with the respective ratio values obtained in normal controls.

The group differences were evaluated using a factorial analysis of variance (ANOVA) with two between-level factors (probable AD and control subjects) and two within-subject factors (cerebral regions, i.e., the ratios obtained for the anatomo-functional areas identified and listed in Table 2, and cerebral hemispheres, i.e., left and right). This analysis was repeated separately for PET and high-resolution SPECT.

An individual analysis was also performed considering ratio values of rCMRglc and counts in each patient as abnormal when beyond the 99% confidence interval of the control group ratio values.

RESULTS

The mean ratio values and standard deviations of PET and high-resolution SPECT regional values of probable AD and normals are reported in Table 2.

For PET studies, the ANOVA showed that both the group effect ($F = 49.9$, $df = 1$, $p < 0.00001$) and the region effect ($F = 21.7$, $df = 6$, $p < 0.00001$) were significant, whereas the hemisphere effect was not significant. The group × region interaction was significant ($F = 12$, $df = 6$, $p < 0.00001$). This was further analyzed by simple main effects which showed high significant difference ($p < 0.0001$) for the associative and mesial frontal cortex, the parietal and temporal cortices, whereas the difference was not significant for the lateral occipital cortex, the thalamus and the cerebellum (Table 2).

For high-resolution SPECT studies, there was a significant difference between groups ($F = 9$, $df = 1$, $p < 0.005$) and between regions ($F = 48$, $df = 6$, $p < 0.00001$), whereas the difference between sides was not significant ($F = 3.2$, $df = 1$, n.s.). The group × region interaction was significant ($F = 3.2$, $df = 6$, $p < 0.005$) and the simple main effects analysis showed significant differences for the parietal ($p < 0.001$) and the temporal ($p < 0.005$) cortices (Table 2). A typical PET and high-resolution SPECT pattern of bilateral temporo-parietal abnormalities is shown in Figure 1.

The results obtained with the individual analysis are represented in Figure 2 where the ratio values of the parietal, temporal and associative frontal cortices of the left and right hemispheres are reported. Metabolism or perfusion were considered abnormal when the regional values (either of the right or left hemisphere or both) were out of

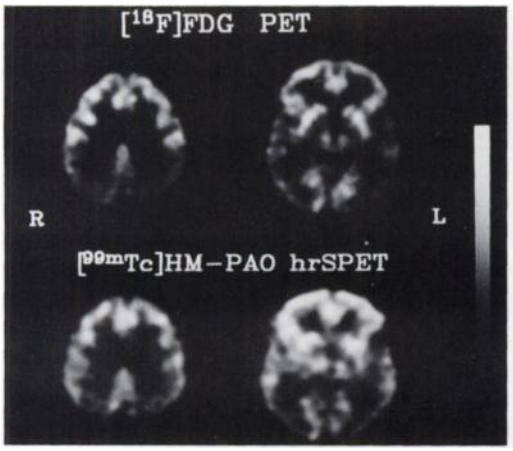

FIGURE 1. Cerebral glucose metabolism using PET with [^{18}F]FDG (top row) and perfusion using high-resolution SPECT with ^{99m}Tc-HMPAO respectively (bottom row) in one patient with probable AD (Patient 3, Table 1). Two tomographic levels parallel to the orbito-meatal line through the mid and cranial parts of the brain are represented. Images are displayed with respect to the maximum value of each study (PET and SPECT). Both studies show marked reduction of metabolism in the temporal and parietal cortices, more marked in the right side. Note the preservation of metabolism and perfusion in the calcarine cortex and in the basal ganglia, which are well depicted in both studies.

the mean ± 2 s.d. of the control group. In the parietal cortex (Fig. 2A) abnormal values were found in all patients by PET and in 16/21 patients by high-resolution SPECT. Of the five patients who did not show areas of hypoperfusion in the parietal cortex at high-resolution SPECT, three showed hypoperfusion in the temporal cortex and the remaining two in the frontal cortex. Areas of hypometabolism and hypoperfusion were also found in the temporal cortex (12/21 with PET and 13/21 with SPECT, Fig. 2B) and in the associative frontal cortex (18/21 with PET and 11/21 with SPECT, Fig. 2C).

The percentage of patients with PET and high-resolution SPECT abnormalities is shown in Table 3. When temporal and parietal regions of the left and right hemispheres were combined, all patients showed hypometabolism with PET and 19/21 (90%) patients showed hypoperfusion with high-resolution SPECT. The two patients who had normal perfusion in the temporo-parietal cortex (#19 and #20; Table 1) showed a selective frontal deficit. PET studies in these patients showed marked abnormalities in the frontal cortex, but also in the parietal lobes (Fig. 3).

As for the presence of interhemispheric asymmetries, unilateral involvement of the temporo-parietal cortex was shown only in one patient (#9) by both PET and high-resolution SPECT, although bilateral abnormalities, more marked on one side, were present in several patients. High-resolution SPECT unilateral involvement of the temporo-parietal cortex was found in two patients (#5 and #12) in whom PET demonstrated bilateral hypometabolism more marked on one side.

DISCUSSION

The results of this study demonstrate that areas of significant reduction of glucose metabolism and blood flow can be detected by PET and high-resolution SPECT, respectively, in the same population of patients with early probable AD. Although the possible relationship between PET metabolic changes and SPECT perfusion changes observed in several neurological disorders, including demen-

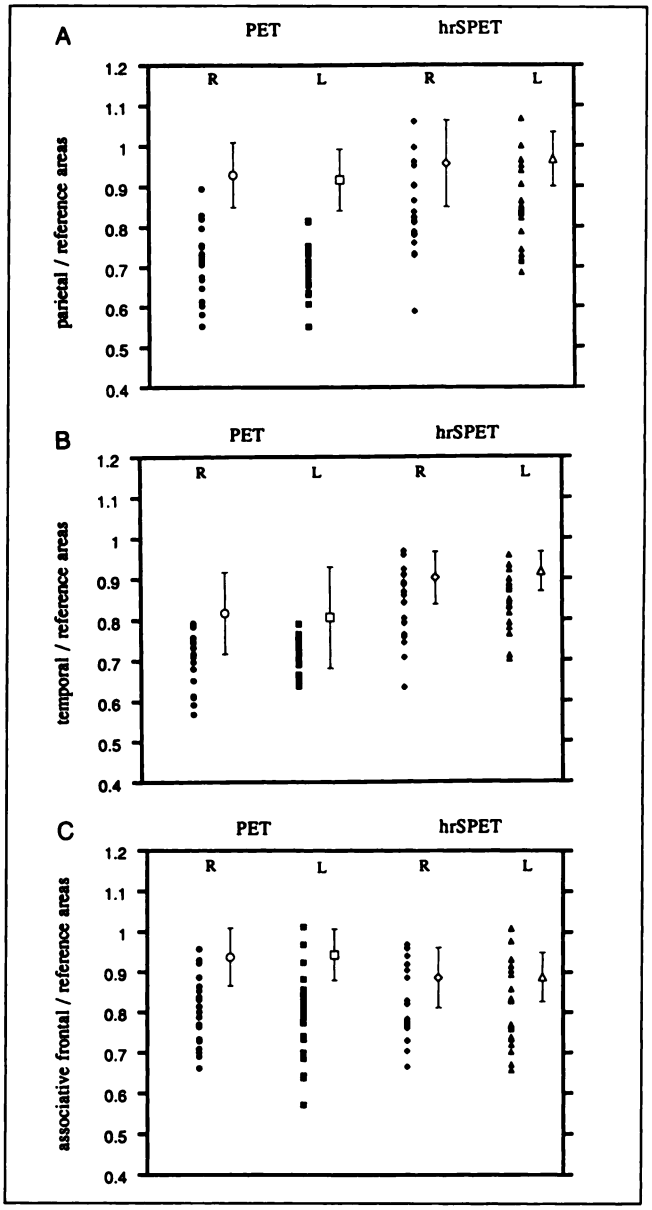

FIGURE 2. Comparison of the relative values of glucose metabolism (PET) and perfusion (high-resolution SPECT) of each single probable AD patient (filled symbols) with the corresponding mean value ±2 s.d. obtained in normal controls (empty symbols) for the two hemispheres. R = right hemisphere; L = left hemisphere. The ratios between mean rCMRglc (for PET) and mean counts (for high-resolution SPECT) in the parietal (A), temporal (B) and associative frontal cortices (C), and mean rCMRglc and counts in the "reference" areas (average of calcarine cortex and basal ganglia) are represented.

TABLE 3
Percent of Patients with Abnormal Regions

Region	PET	SPECT
Associative frontal	86%	52%
Mesial frontal	62%	24%
Temporal	62%	62%
Parietal	100%	76%
Lateral occipital	33%	28%
Temporo/parietal	100%	90%

tia, has been raised (*13,34*), the present study reports a systematic comparison of the same series of patients with probable AD examined with PET and high-resolution SPECT techniques.

Significant differences between probable AD and controls were found in the parietal and temporal cortices both with PET and high-resolution SPECT. The finding of abnormalities in the temporo-parietal cortex, present in all patients by PET, demonstrates the ability of this technique to detect a metabolic pattern which is characteristic of probable AD, consistent with previous reports (*14–16*). Recently, the sensitivity of PET with ^{15}O-water to detect bilateral abnormalities in the temporo-parietal cortex has been reported to be 38% by Powers et al. (*21*) in a population of probable AD patients similar or even more compromised than the one in the present report. However, in the study by Powers et al., the spatial resolution of the images (18 mm FWHM) was lower in comparison with that of the present PET (6.3 mm FWHM) and high-resolution SPECT (8.4 mm FWHM) studies because of factors related to the tracer and PET technology. Furthermore, results and conclusions were drawn only from visual analysis.

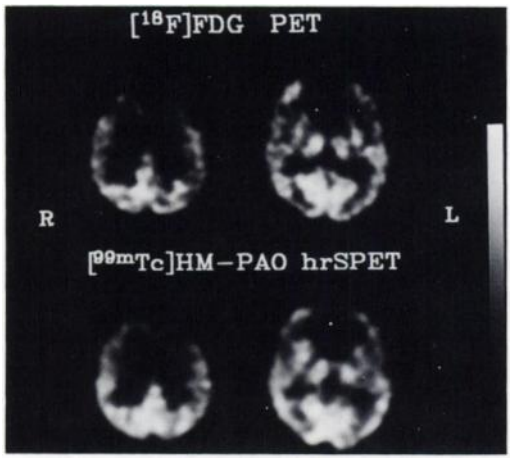

FIGURE 3. Regional glucose metabolism obtained with PET and [^{18}F]FDG (top row) and perfusion obtained with high-resolution SPECT and [^{99m}Tc]HMPAO (bottom row) in Patient 19 (Table 1). Two tomographic levels parallel to the orbito-meatal line through the mid and cranial parts of the brain are represented. Images are displayed with respect to the maximum value of each study (PET and SPECT). Both studies show hypometabolism and hypoperfusion bilaterally in the frontal cortex. PET also shows hypometabolism of the parietal cortex bilaterally.

In this study, abnormalities in the temporo-parietal cortex were also detected by high-resolution SPECT in a high percentage of patients (90%), which is in the range of previously published data (from 70% to 100%) (*35*). The only two patients with a prevalent frontal hypoperfusion on SPECT showed cortical hypometabolism more marked in the frontal areas, but diffuse also on the temporo-parietal areas on PET. In these two cases, Pick's disease or frontal type dementia cannot be excluded, and the differential diagnosis between Pick's and AD is based only on autopsy findings.

The high sensitivity observed in this report might be related to the availability of high spatial resolution PET and SPECT systems and to the use of semiquantitative analysis, such as the ratio analysis reported here.

The anatomical structure most frequently used for the semiquantitative ratio analysis of SPECT studies is the cerebellum (*3–5*). In this study, the reference area used in the ratio was the average activity of the basal ganglia and the calcarine cortex. We did not choose the cerebellum as a reference area because of an apparent uncoupling between perfusion and glucose metabolism in the cerebellar hemispheres. In fact, an overestimation of perfusion obtained with ^{99m}Tc-HMPAO in the cerebellum compared with blood flow estimated with ^{18}F-fluoromethane and PET has been previously reported and it has been attributed to the high capillarity density in the cerebellum (*36*). Furthermore, a cerebral blood flow (CBF) and cerebral metabolic rate for oxygen ($rCMRO_2$) higher than glucose metabolism in normal cerebellum measured with PET has also been reported by Sasaki et al. (*37*). Although a comparative analysis between PET and high-resolution SPECT values in normal regions was not performed because out of the purposes of the present work, an indication of higher values of blood flow estimated with ^{99m}Tc-HMPAO in the cerebellum can be inferred by the data shown in Table 2 where the ratio value of cerebellum in controls measured with high-resolution SPECT was 26% higher than the corresponding value measured with PET.

The calcarine cortex and basal ganglia were chosen because they are usually spared in AD (*33*) and because the use of these structures in the ratios has been recently tested in a PET/FDG study of AD and nonAD patients (*38,39*) and its diagnostic power has been found to be high (sensitivity of 92% and specificity of 80%).

A discrepancy between PET and high-resolution SPECT findings was observed in the detection of abnormalities in the frontal associative cortex. Whereas in the group analysis, PET metabolic values showed that both the lateral and mesial frontal cortex was significantly affected in probable AD, high-resolution SPECT regional variations in the frontal cortex, although present in some of the patients, did not reach a statistical significance in the group analysis. On the other hand, in the parietal cortex, abnormalities were detected by high-resolution SPECT in a smaller number of patients than by PET (Table 3). Although the defect in the temporal and the parietal cortex is severe and constant

enough to reach a statistical significance with both techniques, the defect in the frontal cortex is less frequent and does not reach a statistical significance with high-resolution SPECT. This finding of a slightly lower sensitivity of high-resolution SPECT compared to PET can be caused by several factors, including physical limitations, such as lower resolution of high-resolution SPECT compared to PET, and biological constraints due to the different kinetics of the tracers used (*12,13*).

PET images were obtained with ^{18}F-FDG, a tracer whose metabolic fate and kinetics are well known. Thus, PET analysis can be done based on data of glucose consumption and the information obtained is directly representative of regional functional activity. For high-resolution SPECT studies, we used ^{99m}Tc-HMPAO, a tracer that is known to be distributed in the brain in proportion to cerebral blood flow. Although models to quantify blood flow with HMPAO have been proposed (*40–42*), they require arterial blood samples and metabolite assays, resulting in a limitation for wide clinical application of SPECT studies of demented patients.

In spite of these discrepancies, our findings of similar patterns of glucose metabolism and perfusion in the same probable AD patients seem to indicate that a tight relationship between blood flow and glucose metabolism is maintained in this disorder, which is consistent with the coupling between blood flow and oxygen metabolism previously demonstrated with PET (*43*).

CONCLUSION

The results of this study confirm that: (1) both PET and high-resolution SPECT identify the characteristic temporoparietal pattern in the same series of probable AD patients, with PET being only marginally more accurate than SPECT; and (2) other abnormalities such as frontal involvement are better evaluated with PET. The high resolution of the systems used as well as the use of either quantitative or semiquantitative analysis of the emission tomography data may contribute to the high sensitivity of the methods. Further development of methods for blood flow quantification may improve the diagnostic accuracy of high-resolution SPECT.

ACKNOWLEDGMENTS

The authors thank Mr. Giuseppe Striano of the Department of Nuclear Medicine, H. San Raffaele for expert technical assistance. This work was supported by a National Research Council grant INV 93-2-365.

REFERENCES

1. Holman BL, Devous MD. Functional brain SPECT: the emergence of a powerful clinical method. *J Nucl Med* 1992;33:1888–1904.
2. Johnson KA, Mueller ST, Walsche TM, English RJ, Holman BL. Cerebral perfusion imaging in Alzheimer's disease: use of single photon emission computed tomography and iofetamine hydrochloride I-123. *Arch Neurol* 1987;44:165–168.
3. Jagust AJ, Budinger TF, Reed BR. The diagnosis of dementia with single-photon emission computed tomography. *Arch Neurol* 1987;44:258–262.
4. Perani D, Di Piero V, Vallar G, et al. Technetium-99m HMPAO-SPECT study of regional cerebral perfusion in early Alzheimer's disease. *J Nucl Med* 1988;29:1507–1514.
5. Burns A, Philpot MP, Costa DC, Ell PJ, Levy R. The investigation of Alzheimer's disease with single photon emission tomography. *J Neurol Neurosur and Psych* 1989;52:248–253.
6. Gemmel HG, Sharp PF, Smith FW, Besson J, Ebmeier K, Davidson J, et al. Cerebral blood flow measured by SPECT as a diagnostic tool in the study of dementia. *Psychiatry Res* 1989;29:327–329.
7. Bonte FJ, Hom J, Tintner R, Weiner MF. Single photon tomography in Alzheimer's disease and the dementias. *Semin Nuc Med* 1990;20:342–352.
8. Holman BL, Johnson KA, Gerada B, Carvalho PA, Satlin A. The scintigraphic appearance of Alzheimer's disease: a prospective study using technetium-99m-HMPAO SPECT. *J Nucl Med* 1992;33:181–185.
9. Ell PJ. Mapping cerebral blood flow [Editorial]. *J Nucl Med* 1992;33:1843–1845.
10. Kouris K, Jarritt PH, Costa DC, Ell PJ. Physical assessment of the GE/CGR neurocam and comparison with a single rotating gamma camera. *Eur J Nucl Med* 1992;19:236–242.
11. Lucignani G, Rossetti C, Ferrario P, et al. In vivo metabolism and kinetics of ^{99m}Tc-HMPAO. *Eur J Nucl Med* 1990;16:249–255.
12. Sorenson JA, Phelps ME. Nuclear medicine tomography: systems and devices. In: Sorenson JA, Phelps ME, eds. *Physics in nuclear medicine, second edition*. Orlando, Florida: Grune & Stratton, Inc.; 1987:424–451.
13. Jagust W, Eberling J. MRI, CT, SPECT, PET: their use in diagnosing dementia. *Geriatrics* 1991;46:28–35.
14. Alavi A, Dann R, Chawluk J, Alavi J, Kushner M, Reivich M. Positron emission tomography imaging of regional cerebral glucose metabolism. *Semin Nucl Med* 1986;16:2–34.
15. Haxby JV, Grady CL, Duara R, Schlageter N, Berg G, Rapoport SI. Neocortical metabolic abnormalities precede nonmemory cognitive defects in early Alzheimer's type dementia. *Arch Neurol* 1986;43:882–885.
16. Kuhl DE, Small GW, Riege WH, et al. Cerebral metabolic patterns before the diagnosis of probable Alzheimer's disease. *J Cereb Blood Flow Metab* 1987;7:S406.
17. Mielke R, Herholz K, Kessler J, Heiss D. Differences of regional cerebral glucose metabolism between presenile and senile dementia of Alzheimer type. *Neurobiology of Aging* 1991;13:93–98.
18. Haxby JV, Duara R, Grady CL, Cutler NR, Rapoport SI. Relations between neuropsychological and cerebral metabolic asymmetries in early Alzheimer's disease. *J Cereb Blood Flow Metab* 1985;5:193–200.
19. McGeer PL, Kamo H, Harrop R, et al. Positron emission tomography in patients with clinically diagnosed Alzheimer's disease. *Can Med Ass J* 1986;134:597–607.
20. Loewenstein D, Yoshii F, Barker WW, et al. Predominant left hemispheric metabolic deficit predicts early manifestation of dementia. *J Cereb Blood Flow Metab* 1987;7:S416.
21. Powers WJ, Perlmutter JS, Videen TO, et al. Blinded clinical evaluation of positron emission tomography for diagnosis of probable Alzheimer's disease. *Neurology* 1992;42:765–770.
22. McKhann G, Drachman D, Folstein M, et al. Clinical diagnosis of Alzheimer's disease: report of the NINCDS-ADRDA Work Group under the auspicies of Department of Health and Human Services Task Force on Alzheimer's disease. *Neurology* 1984;34:939–944.
23. Spinks TJ, Jones T, Gilardi MC, Heather JD. Physical performance of the latest generation of commercial positron scanner. *IEEE Trans Nucl Sci* 1988;35:721–725.
24. Bettinardi V, Scardaoni R, Gilardi MC, et al. Head holder for PET, CT and MRI studies. *J Comput Assist Tomogr* 1991;15:886–892.
25. Hamacher K, Cohenen HH, Stocklin G. Efficient stereospecific synthesis of no-carrier-added 2-[18F]fluoro-2-deoxy-D-glucose using aminopolyether supported nucleophilic substitution. *J Nucl Med* 1986;27:235–238.
26. Sokoloff L, Reivich M, Kennedy C, et al. The ^{14}C deoxyglucose method for the measurement of local cerebral glucose utilization: theory, procedure and normal values in the conscious and anesthetized albino rat. *J Neurochem* 1977;28:897–916.
27. Reivich M, Alavi A, Wolf A, et al. Glucose metabolic rate kinetic model parameter determination in humans: the lumped constants and rate constants for [^{18}F]fluorodeoxyglucose and [^{11}C]deoxyglucose. *J Cereb Blood Flow Metab* 1985;5:179–192.
28. Genna S, Smith AP. The development of ASPECT, an annular single crystal brain camera for high efficiency SPECT. *IEEE Trans Nucl Sci* 1988;NS-35:654–658.
29. Chang LT. A method for attenuation correction in radionuclide computed tomography. *IEEE Trans Nucl Sci* 1978;NS-25:638–643.

30. Damasio H, Damasio AR. *Lesion analysis in neuropsychology*. New York: Oxford University Press, 1989.
31. Cappa SF, Perani D, Bressi S, Paulesu E, Franceschi M, Fazio F. Crossed aphasia: a PET follow-up study of two cases. *J Neurol Neurosurg Psychiatry* 1993;56:665–671.
32. Pantano P, Di Piero V, Ricci M, Fieschi C, Bozzao L, Lenzi GL. Motor stimulation response by technetium-99m-hexamethylpropylene amine oxime split-dose method and single photon emission tomography. *Eur J Nucl Med* 1992;19:939–945.
33. Brun A, Englund E. Regional pattern of degeneration in Alzheimer's disease: neuronal loss and histopathological grading. *Histopathology* 1981;5: 549–564.
34. Maurer AH. Nuclear medicine: SPECT comparison to PET. *Radiol Clin North Am* 1988;26:1059–1074.
35. Dewan M, Gupta S. Toward a definite diagnosis of Alzheimer's disease. *Comprehensive Psychiatry* 1992;33:282–290.
36. Heiss WD, Herholz K, Podreka I, Neubauer I, Pietrzyk U. Comparison of ^{99m}Tc-HMPAO SPECT with ^{18}F-fluoromethane PET in cerebrovascular disease. *J Cereb Blood Flow Metab* 1990;10:687–697.
37. Sasaki H, Kanno I, Murakami M, Shishido F, Uemura K. Tomographic mapping of kinetic rate constants in the fluorodeoxyglucose model using dynamic positron emission tomography. *J Cereb Blood Flow Metab* 1986; 6:447–454.
38. Herholz K, Adams R, Kessler J, Szeliers B, Grond M, Heiss WD. Criteria for the diagnosis of Alzheimer's disease with positron emission tomography. *Dementia* 1990;1:156–164.
39. Heroltz K, Perani D, Salmon E, Franck G, Fazio F, Heiss WD, Comar D. Comparability of FDG PET studies in probable Alzheimer's disease. *J Nucl Med* 1993;34:1460–1466.
40. Lassen NA, Andersen AR, Friberg L, Paulson OB. The retention of ^{99m}Tc-d,l-HMPAO in the human brain after intracarotid bolus injection: a kinetic analysis. *J Cereb Blood Flow Metab* 1988;8:S13–S22.
41. Matzuda H, Oba H, Seki H, et al. Determination of flow rate constants in a kinetic model of ^{99m}Tc-hexamethyl-propilene amine oxime in the human brain. *J Cereb Blood Flow Metab* 1988;8:S61–S68.
42. Pupi A, De Cristofaro MTR, Bacciottini L, et al. An analysis of the arterial input curve for technetium-99m-HMPAO: quantification of rCBF using single-photon emission computed tomography. *J Nucl Med* 1991;32:1501–1506.
43. Frackowiack RSJ, Pozzilli C, Legg NNJ, et al. Regional cerebral oxygen supply and utilization in dementia: a clinical and physiological study with oxygen-15 and positron tomography. *Brain* 1981;104:753–778.